ALCHEMY Jurnal Penelitian Kimia

Official Website: https://jurnal.uns.ac.id/alchemy

ISSN 1412-4092
EISSN 2443-4183

Synthesis, Characterization, and DFT Computational Study of Cu(II) Complex with 3-Hydroxybenzoate

Fastabiqul Khoirot, Muhammad David Julian Syach, Sentot Budi Rahardjo*, Triana Kusumaningsih

Department of Chemistry, Faculty of Mathematics and Natural Sciences, Sebelas Maret University
Jalan Ir. Sutami 36 A, Kentingan, Surakarta, 57126, Indonesia

**Corresponding author: sentotbr@staff.uns.ac.id*

DOI: 10.20961/alchemy.22.1.114305.106-116

Received 9 January 2026, Revised 19 February 2026, Accepted 26 February 2026, Published 31 March 2026

Keywords:

3-hydroxybenzoic; complex characterization; computational studies; Cu(II) complex; synthesis.

ABSTRACT. This study focuses on the synthesis, characterization, and density functional theory (DFT) computational study of Cu(II) complexes with 3-hydroxybenzoic acid ligands. The synthesis process was carried out by reacting $CuCl_2 \cdot 2H_2O$ with 3-hydroxybenzoic acid ligands in methanol, refluxing for 3 hours, and allowing the mixture to stand until complex precipitation formed. The complex formula was determined by atomic absorption spectrometry (AAS), thermogravimetric analysis (TGA), and molar conductivity measurements (41 $S \cdot cm^2 \cdot mol^{-1}$), indicating that Cl^- acts as a counterion and that the complex formula is $[Cu(3\text{-hydroxybenzoate})_2]Cl_2 \cdot 4H_2O$. The complex exhibits a single electronic absorption peak at 914 nm, indicating ligand-metal charge transfer (LMCT) and d-d transitions, consistent with a distorted square-planar geometry. The infrared spectrum shows a phenolic –OH band, indicating that –OH is not deprotonated. Computational methods were used to reveal the electronic structure and molecular geometry, and to verify the experimental data. This complex forms a distorted square planar structure.

INTRODUCTION

Complex compounds are compounds formed from covalent bonds of coordination between metals as central atoms and ligands as electron donors (Devi *et al*., 2019). The synthesis of complex compounds involving various metals with mono-, bi-, or multidentate ligands can yield a wide range of structures and applications in everyday life (Bhowmick *et al*., 2019). The synthesis of low-toxicity metal complexes, based on their structures and reactivities, provides a model for many researchers in the field of coordination chemistry (Ashouri *et al*., 2020). The application of complex compounds depends on the selection system of the type of metal and ligand used, including structure, complex geometry, oxidation state, stability, and solubility (Karges *et al*., 2021). Several factors affect complex synthesis, namely solvent type, temperature, and pH. When the temperature is increased along with the appropriate pH, the complex forms efficiently (Ostellari *et al*., 2025).

Transition metal complexes with aromatic carboxylic acid ligands have attracted significant attention in modern coordination chemistry due to their important role in a wide range of applications, from catalysts to functional materials and bioactive agents (Yadav *et al*., 2025). Copper(II) is a transition metal with high abundance and unique redox properties, forming stable complexes with a variety of oxygen and nitrogen donor ligands, exhibiting coordination geometries ranging from tetrahedral to octahedral (Valach *et al*., 2010). 3-hydroxybenzoate (3HBA) is an interesting bidentate ligand due to its ability to form chelate structures through carboxylate groups while providing additional hydroxyl groups for secondary interactions. The complex compound Cu(II)-3-hydroxybenzoate can be applied to various fields, including biological activity (antibacterial, anticancer, antioxidant), catalysis, and computational studies.

Computational studies using density functional theory (DFT) have become an invaluable tool for understanding the electronic, structural, and complex reactivity properties of transition metals (Akbari *et al*., 2024). The DFT method, especially with hybrid functionals such as B3LYP with dispersion correction, can provide accurate predictions of molecular geometry, electronic parameters such as HOMO-LUMO energy gaps, and

Cite this as: Khoirot, F., Syach, M. D. J., Rahardjo, S. B., and Kusumaningsih, T. (2026). Synthesis, Characterization, and DFT Computational Study of Cu(II) Complex with 3-Hydroxybenzoate. *ALCHEMY Jurnal Penelitian Kimia*, 22(1), 106-116. doi: https://dx/doi.org/10.20961/alchemy.22.1.114305.106-116.

Copyright © 2026, Universitas Sebelas Maret, ISSN 1412-4092, e ISSN 2443-4183

properties of coordination complex spectroscopy (Amin *et al*., 2025). Molecular frontier orbital analysis (HOMO and LUMO) is essential for understanding the kinetic stability, chemical reactivity, and charge-transfer mechanisms in transition-metal complexes (Hasanova *et al*., 2023).

The characterization of ligand-to-metal charge transfer (LMCT) in copper complexes is particularly relevant to understanding their photochemical and catalytic properties (Juliá, 2022). The LMCT transition involves the transfer of electrons from the fully occupied ligand orbital to the empty or partially filled metal d orbital, resulting in intense absorption bands in the UV-Vis spectrum (May and Dempsey, 2024). Cu(II) complexes with aromatic carboxylate ligands often exhibit characteristic LMCT transitions that can affect their catalytic and photochemical activity.

This study aims to comprehensively investigate the electronic structure, geometric parameters, and reactivity properties of Cu(II) complexes with 3-hydroxybenzoate using the DFT method. Special focus is given to HOMO-LUMO analysis to understand stability and reactivity, characterization of dominant electronic transitions, and mapping of electrostatic charge distribution via Molecular Electrostatic Potential (MEP). The results of this study are expected to provide fundamental insights into the complex structure-property relationships of Cu-3HBA that can contribute to the development of copper-based materials for catalytic and functional applications.

RESEARCH METHODS

The ingredients used in this study were 3-hydroxybenzoate, $CuCl_2 \cdot 2H_2O$, methanol, DMSO, HNO_3 69%, dry KBr, $CuCl_2 \cdot 2H_2O$, $Cu(NO_3)_2 \cdot 3H_2O$, $Cu(SO_4)_2 \cdot 5H_2O$, $CoSO_4 \cdot 7H_2O$, $CoCl_2 \cdot 6H_2O$, $FeSO_4 \cdot 7H_2O$, NaCl from E. Merck and Sigma-Aldrich.

Synthesis of Cu(II) Complex

$CuCl_2 \cdot 2H_2O$ (0.1705 g; 1 mmol) was dissolved in methanol (5 mL), and 3-hydroxybenzoic acid (0.27625 g; 2 mmol) was dissolved in methanol (5 mL). Then, a solution of $CuCl_2 \cdot 2H_2O$ (0.1705 g; 1 mmol) was added dropwise to a stirred solution of 3-hydroxybenzoic acid, and the mixture was refluxed for 3 hours. The solution was left to settle at room temperature for 3 days to form complex deposits; the deposits were then filtered and vacuum-dried.

Characterization of Cu(II) Complex Analysis

Indications of complex formation are characterized by a shift in the maximum of absorption towards shorter wavelengths using the 'Lambda 25 Perkin Elmer' UV-Vis spectrophotometer. The purity of the complex was determined using the Atomic Absorption Spectrophotometer (AAS) 'Shimadzu AA-6650'. The 'Diamond Perkin Elmer' Thermogravimetry Analyzer/Differential Thermal Analyzer (TG/DTA) is used for the determination of the water content in the complex. The ratio of cation and anion charges is determined by measuring conductivity. Complex electricity was performed using a conducttometer 'Jenway CE 4071' at a complex concentration of 1×10^{-3} M. Atoms or atomic groups coordinated on Cu(II) ions were estimated from infrared data using the 'Prestige-21 Shimadzu' Fourier Transform Infrared (FTIR) spectrophotometer in the range of 400 – 4000 cm^{-1}.

Computational Studies

All quantum chemistry calculations were performed using the ORCA software package version 6.1.0 (Neese, 2012; Neese *et al*., 2020). The calculation was performed within the framework of Density Functional Theory (DFT) with the functional hybrid B3LYP (Becke, 1993; Lee *et al*., 1988), supplemented with an empirical system correction D3 using Becke-Johnson (BJ) (B3LYP-D3BJ) to accurately account for van der Waals interactions and long-range system forces (Grimme *et al*., 2010; Grimme *et al*., 2011). Functional B3LYP is one of the most 107versatile methods. It has been shown to provide accurate results for the quantum properties of transition metal complexes, including the HOMO-LUMO energy gap (Mohamed *et.al*., 2025).

Different set bases were applied to accommodate the different electronic characteristics of atoms: the Carbon (C), Oxygen (O), and Hydrogen (H) atoms are represented by the Pople 6-311+G(d,p) set base (Krishnan *et al*., 1980), while the double-polarized triple-zeta valence plus polarization set base, def2-TZVPP, is used for the Copper (Cu) transition metal atom (Weigend and Ahlrichs, 2005). Selecting a larger basis set for transition metals is essential for accurately describing complex electronic and d-orbital properties (Grau *et al*., 2024). Computational efficiency is improved by using the Resolution of the Identity (RI) approach with an auxiliary basis set def2/J,

Copyright © 2026, Universitas Sebelas Maret, ISSN 1412-4092, e ISSN 2443-4183

uniformly applied to all atoms in the system (Weigend, 2006). The LARGEPRINT command produces complete and detailed output.

RESULTS AND DISCUSSION

Synthesis of Cu(II) Complex

Synthesis of Cu(II)-3-hydroxybenzoate complexes with a 1:2 metal-ligand mole ratio yields dark green deposits (0.417 g; 86.51%). The formation of the complex is confirmed by a shift in the UV-Vis maximum absorption wavelength from 944 nm to 914 nm (Figure 1). This shift occurs because the H_2O molecule coordinated on the Cu(II) ion is replaced by a ligand of 3-hydroxybenzoic acid, which has a higher ligand strength compared to H_2O. The presence of a λmax shift is also found in $[Cu(3\text{-picolylamine})_4]SO_4.5H_2O$, which undergoes a shift in the electron spectrum towards a smaller wavelength from 815 nm to 751 nm (Azizah *et al*., 2025).

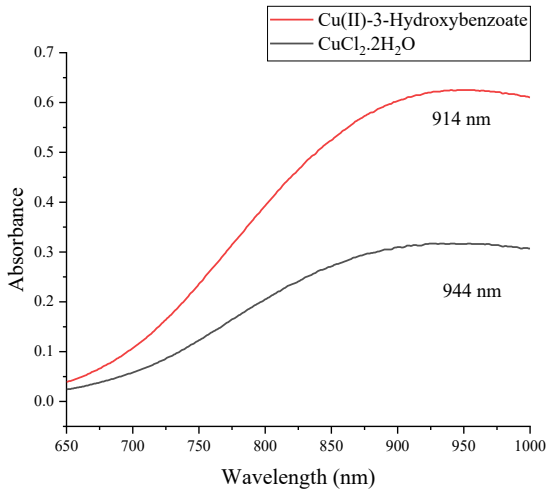


Figure 1. Electron spectrum of $CuCl_2 \cdot 2H_2O$ and Cu(II)- 3-Hydroxybenzoate in DMSO.

Determination of Complex Formulas

Copper Content Analysis

The copper content in the Cu(II)-3-hydroxybenzoate complex is 13.17 ± 0.03% shown in Table S1. The experimental copper content is compared with theoretical values for various complex formulas, as shown in Table 1. Based on Table 1, the Cu(II)-3-hydroxybenzoate complex is estimated to have the chemical formula Cu(3-hydroxybenzoate)$_2Cl_2 \cdot nH_2O$ (n = 3, 4, or 5).

Table 1. The theoretical copper content of Cu(II)-3-hydroxybenzoate.

Complex Formulas	Molecular Weight (g/ mol)	Theoretical Copper Content (%)
Cu(3-hydroxybenzoate)$_2Cl_2$	410.67	15.47
Cu(3-hydroxybenzoate)$_2Cl_2 \cdot H_2O$	428.70	14.82
Cu(3-hydroxybenzoate)$_2Cl_2 \cdot 2H_2O$	446.72	14.22
Cu(3-hydroxybenzoate)$_2Cl_2 \cdot 3H_2O$	464.73	13.67
Cu(3-hydroxybenzoate)$_2Cl_2 \cdot 4H_2O$	**482.75**	**13.16**
Cu(3-hydroxybenzoate)$_2Cl_2 \cdot 5H_2O$	500.76	12.69
Cu(3-hydroxybenzoate)$_2Cl_2 \cdot 6H_2O$	518.78	12.25

Thermal Analysis

Thermal analysis of the Cu(II)-3-hydroxybenzoate complex in the calculations of Table S2 and Figure 2 shows one stage of mass loss. The first stage, a 13.58% loss, occurred between 30 – 110 °C, corresponding to the release of 4 water molecules (H_2O). Mass loss in the temperature range of 30 – 130 °C indicates the loss of water molecules as crystalline water (not coordinated with the central metal), while mass loss in the range of 150 – 200 °C indicates the loss of water molecules from ligands (Rasyda *et al*., 2021). Once the 3HBA ligand is decomposed, all that remains is a mixture of Cu/Cu_2O and carbon (C). Oxygen residues can react with Cu residues (such as Cu or Cu_2O from ligand decomposition) and will oxidize into heavier CuO as they bind to oxygen. An increase in

Copyright © 2026, Universitas Sebelas Maret, ISSN 1412-4092, e ISSN 2443-4183

mass at 600 °C allows the presence of CuO (Domán *et al*., 2017). The research by Aly *et al*. (2024) reported increases in mass at 620 °C and 790 °C, indicating the formation of CuO and carbon (C). Therefore, the Cu(II)-3-hydroxybenzoate complex contains 4 molecules of crystalline water, thus producing the molecular formula Cu(3-hydroxybenzoate)$_2$Cl$_2$·4H$_2$O with a molecular weight of 482.746 g/mol.

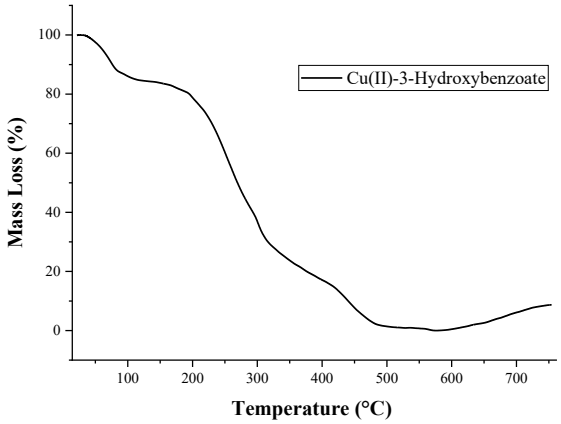


Figure 2. Spectrum of thermal analysis of Cu(II)-3-Hydroxybenzoate complex.

Conductivity Measurement

Measurements of the electrical conductivity of Cu(II)-3-hydroxybenzoate complexes with multiple standard solutions in DMSO (1× 10-3 M) are presented in Table 2. The electrical conductivity values of the Cu(II)-3-hydroxybenzoate complex that are close to the values of NiCl$_2$·6H$_2$O and Ni(NO$_3$)$_2$·6H$_2$O indicate that the complex contains three ions with a cation and anion charge ratio of 1:2. This suggests that the complex functions as an electrolyte, with the Cl$^-$ ion acting as a counterion. Therefore, the approximate molecular formula for the Cu(II)-3-hydroxybenzoate complex is [Cu(3-hydroxybenzoate)$_2$]Cl$_2$·4H$_2$O.

Table 2. Measurement of the electrical conductivity of the Cu(II)-3-hydroxybenzoate complex with multiple standard solutions in DMSO.

Solution	Λ*m (S.cm^2/mol)	Number of Ions
DMSO	0	-
CoSO$_4$·7H$_2$O	10	2
CuSO$_4$·5H$_2$O	9	2
Ni(NO$_3$)$_2$·6H$_2$O	**40**	**3**
NiCl$_2$·6H$_2$O	**41**	**3**
Fe(NO$_3$)$_3$·9H$_2$O	59	4
[Cu(3-hydroxybenzoate)$_2$]Cl$_2$·4H$_2$O	**41**	**3**

Infrared Spectral Measurements

The FTIR spectrum of the ligand and Cu(II)-3-hydroxybenzoate complex (Figure 3) shows a shift at the peak of absorption of the functional group of the 3-hydroxybenzoate ligand when binding to Cu(II), as shown in Table 3. The shift ν(O–H) from 3288 cm^{-1} to 3280 cm^{-1}. The C=O bond shifts from 1695 cm^{-1} to 1719 cm^{-1}. The IR spectrum of the Cu(II)-3-hydroxybenzoate complex shows a new band at 438 cm^{-1}, assigned to the Cu–O bond vibration. The wide band around 3400 – 3200 cm^{-1} is a typical band of O–H strains, the width of which strongly indicates *overlapping* between the phenolic –OH of 3-hydroxybenzoate and –OH of 4 crystalline H$_2$O molecules. The absence of drastic shifts or loss of phenolic –OH bands indicates that the –OH group is not deprotonated.

Table 3. Absorption of functional groups of complex compounds Cu(II)-3-hydroxybenzoate and 3-hydroxybenzoate.

Functional Groups	Theory (cm^{-1})	Number of Experimental Waves (cm^{-1})	
		Ligand	Complex
O–H	3696 – 3367 (Ermiş and Durmuş, 2020)	3288	3280
C=O	1688 (Bhaskar *et al*., 2020)	1695	1719
Cu–O	425 (Kargar *et al*., 2021)	-	438

Copyright © 2026, Universitas Sebelas Maret, ISSN 1412-4092, e ISSN 2443-4183

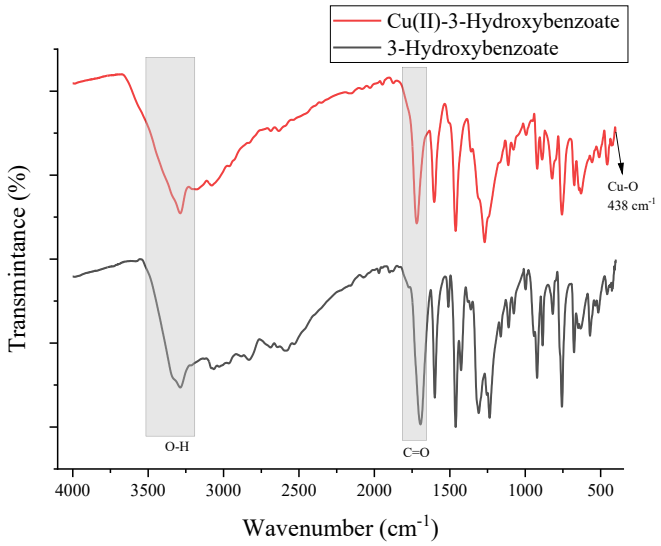


Figure 3. FTIR Spectrum of Cu(II)-3-hydroxybenzoate and 3-hydroxybenzoate complexes.

Electronic Spectrum Measurement

The results of the electronic spectrum measurements can be seen in Table 4, which shows that the molar absorbivity (ε) of the complex $[Cu(3\text{-hydroxybenzoate})_2]Cl_2{\cdot}4H_2O$ is greater than that of $CuCl_2{\cdot}2H_2O$ which has a greater molar absorbivity value (ε) after coordination, and this indicates the presence of a typical d-d transition for *distorted* planar square geometry (El-Deen *et al*., 2018). Molar absorbivity (ε) is related to the type of electronic transition. This relates to the increase in covalent bond properties resulting from the mixing of d and π orbitals.

Table 4. Electronic spectrum measurements.

No.	Compounds	λ_{max} (nm)	A	υ (cm^{-1})	ε ($L.mol^{-1}.cm^{-1}$)
1.	$CuCl_2{\cdot}2H_2O$	944	0.364	10593	36
2.	$[Cu(3\text{-hydroxybenzoate})_2]Cl_2{\cdot}4H_2O$	914	0.643	10940	145

The absorptivity value (ε) of 146 $L.mol^{-1}.cm^{-1}$ in the Cu(II) complex indicates that the observed absorption band is derived from the d-d transition. In Cu(II) complexes with distorted planar square geometry, the Laporte rule does not apply strictly due to the absence of an inversion center and the structural distortion associated with the Jahn-Teller effect. This condition increases mixing of metal and ligand orbitals, so that the theoretically forbidden d-d transition is partially permitted, reflected in values in the hundreds range. The mixing of the d and π orbitals is also evident in the DFT orbital visualization. Mixing of d and π orbitals can lower the "prohibition" on electronic transitions, so that the transition from HOMO localized in ligand π systems to LUMO that has a strong Ligand to Metal Charge Transfer (LMCT) character.

Based on crystal field theory, the strength of the ligand field () is proportional to the energy (E). Meanwhile, according to Planck's Law, energy is proportional to frequency (v), where the frequency is inversely proportional to the wavelength (λ), so that a strong ligand field results in a smaller wavelength (λ) and a greater energy (E). The relationship of energy (E) and wavelength (λ) obtained by Planck's Law can be seen in the Δ_0 Table 5.

Table 5. Calculations based on Planck's Law.

No.	Compounds	λ (m)	υ (cm^{-1})	E (Joule)
1.	$CuCl_2{\cdot}2H_2O$	944×10^{-9}	10593,22	7.02×10^{-30}
2.	$[Cu(3\text{-hydroxybenzoate})_2]Cl_2{\cdot}4H_2O$	914×10^{-9}	10940,92	7.25×10^{-30}

Structure Geometry Optimization Results

The results of the structural optimization of $Cu(3\text{-hydroxybenzoate})_2]Cl_2{\cdot}4H_2O$ indicate that the Cu(II) coordination center adopts a distorted planar square geometry with four oxygen atoms as the main donors, as shown in Figure 4. Planar square geometry is a common configuration in Cu(II) complexes with d^9 ions, although distortion from the ideal geometry often occurs due to ligand-electron and steric effects (Grau *et al*., 2024; Matović *et al*., 2000). The geometric distortion in this complex is reflected in the fairly significant variation in bond angles,

Copyright © 2026, Universitas Sebelas Maret, ISSN 1412-4092, e ISSN 2443-4183

as shown in Table 6, where the two narrow angles, O1-Cu-O2 and O4-Cu-O5, are about 65.9°, while the angles O1-Cu-O5 and O2-Cu-O4 are about 114°.

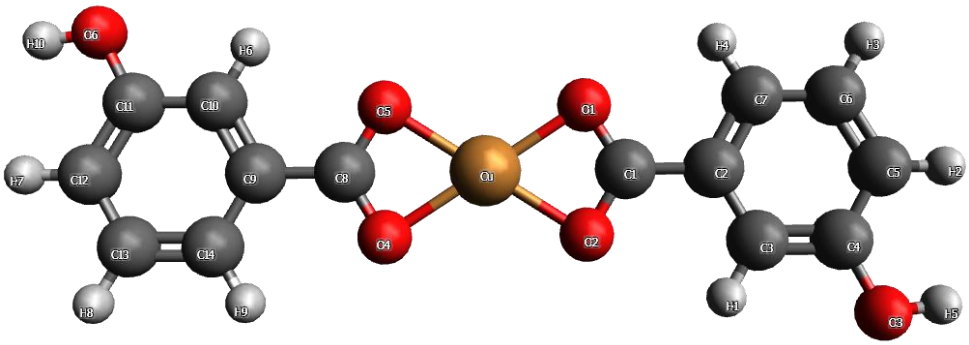


Figure 4. Visualization of Cu(II) complex structures with 3HBA.

Table 6. Bond angles in Cu(3-hydroxybenzoate)$_2$]Cl$_2$·4H$_2$O.

Bonding	Angle (°)
O1-Cu-O2	65.9
O1-Cu-O5	114.0
O2-Cu-O4	114.1
O4-Cu-O5	65.9
O1-C1-O2	116.9
O4-C8-O5	116.9

The angular pattern indicates a chelating configuration of the ligands, forcing the donor atoms into an orientation that is not completely symmetrical, as shown in Table 6. The narrow chelate angle (65.9°) is a typical characteristic of a five-member chelate system formed by a carboxylate group that binds to the metal in bidentate mode. The deviation from the ideal planar square geometry (90° angle) can be attributed to intramolecular steric factors and the electronic effects of aromatic ligands (Sabolović *and* Liedl, 1999). The internal angles of the two carboxylate groups, O1-C1-O2 and O4-C8-O5, are 116.9°, respectively, corresponding to the sp² geometric character common to delocalized carboxylate systems. These angular values are consistent with experimental crystallographic data for copper carboxylate complexes reported in the literature.

Table 7. Bond length in Cu(3-hydroxybenzoate)$_2$]Cl$_2$·4H$_2$O.

Bonding	Length (Å)	Bonding	Length (Å)
Cu-O1	2.001	C1-O1	1.276
Cu-O2	1.996	C1-O2	1.276
Cu-O3	2.003	C8-O4	1.276
Cu-O4	1.998	C8-O5	1.276

The length of the Cu–O bond is in the range of 1.996 – 2.003 Å, indicating a relatively balanced coordination interaction between the metal center and the oxygen atom. This bond length is within the typical range for Cu(II)-carboxylate complexes and indicates moderate coordinating bond strength (Valach *et al*., 2010). The length of the C–O bond in the ligands remains consistent at about 1.276 Å, reflecting the delocalization of electrons in stable carboxylate groups. The uniformity of the length of the C–O bond indicates that the two 3HBA ligands make an equivalent electronic contribution to the Cu(II) metal center.

Further calculations indicate that the formation of the Cu(II)–3HBA complex in the gas phase is highly energetically favorable. The complexation energy is calculated as the difference in electronic energy between the complex and its separate species (Cu(II) ions and two 3-HBA ligands), yielding -1.0424 Hartree, or about -654.12 kcal/mol. This large negative value indicates a significant decrease in total energy, making the complex very electronically stable. Since it is carried out in the gaseous phase without the solvent effect, the entire stabilization contribution comes from the direct interaction of the metal-ligand, especially the coordination bond through the donation of electron pairs from the ligand donor atom atom to the empty orbital of the metal as well as the

Copyright © 2026, Universitas Sebelas Maret, ISSN 1412-4092, e ISSN 2443-4183

electrostatic interaction, so that the binding strength obtained represents the maximum intrinsic stabilization of the system.

Overall, these structural parameters confirm that the Cu (3-h*y*dro*xy*benzoat*e*)$_2$]Cl_2·4H_2O complex has a stable coordination architecture, with typical distortions arising from the formation of chelate rings. The optimized structure shows that the complex maintains structural integrity through the formation of strong chelates, which are essential for its thermal and chemical stability in practical applications.

HOMO-LUMO Analysis

The HOMO-LUMO energy gap is a fundamental parameter that describes a molecule's kinetic stability and chemical reactivity (Huang *et al*., 2017). The energy gap of the Cu(II) complex with 3-hydroxybenzaoic acid (3HBA) is 4.772 eV. In general, the greater the energy gap value, the more kinetically stable a molecule will be and the less reactive it will be to chemical reactions, as it takes more energy to promote electrons from HOMO to LUMO (Miar *et al*., 2021). In contrast, small energy gaps indicate molecules that are more reactive and prone to electronic transitions.

The value of 4.772 eV indicates that this complex has moderate kinetic stability. For transition-metal complexes, energy gaps of 3 – 5 eV generally indicate a balance between stability and reactivity that is adequate for catalytic applications (Akbari *et al*., 2024). This relatively large energy implies that the complex does not undergo oxidation or reduction easily under standard conditions and requires a sufficiently high activation energy to react.

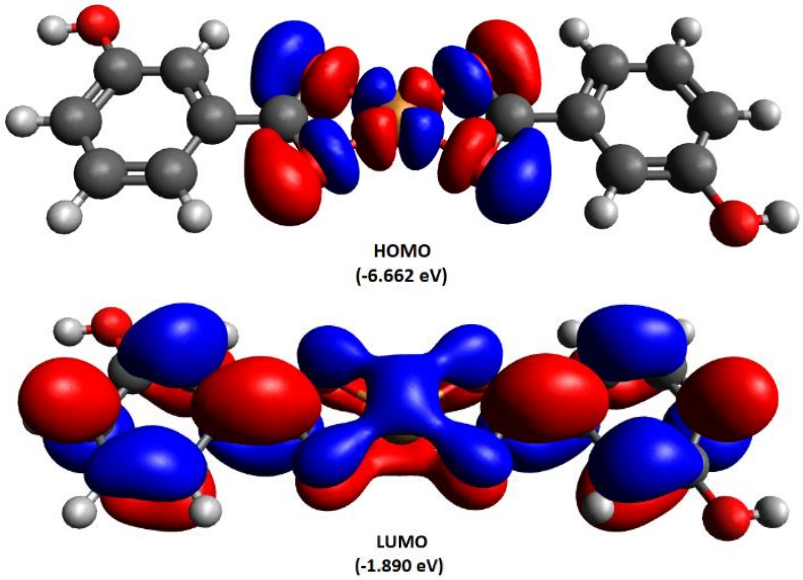


Figure 5. Visualization of HOMO and LUMO of Cu(II) complexes with 3HBA.

Meanwhile, the orbital visualization in Figure 5 shows the dominant primary electronic transition. HOMO (-6,662 eV) is significantly localized to organic ligands (π-orbitals), making it an electron donation center (nucleophilic). In contrast, LUMO (-1.890 eV) has a major contribution to the Cu(II) metal center and the coordinating oxygen atom (mixed π*/d-orbital), making it an electron acceptor center (electrophilic).

The lowest energy electronic transition (HOMO→LUMO) is the Ligand-to-Metal Charge Transfer (LMCT) type, in which electrons move from the ligand to the center of the metal. These LMCT transitions are crucial for explaining the optical activity and catalytic properties of the complex, which often involve the absorption of UV-Vis light to trigger this charge transfer (May and Dempsey, 2024; Juliá, 2022).

LMCT transitions in Cu(II) complexes with carboxylate ligands have been reported to produce intense absorption bands because they are not constrained by Laporte's selection rules like d-d transitions (Juliá, 2022). LMCT transitions can facilitate the activation of complex photochemicals and generate reactive species useful for catalytic applications. In the context of the Cu-3HBA complex, the LMCT transition that occurred at an energy of 4.772 eV (about 260 nm) was within the UV range, which is consistent with the absorption bands characteristic of the aromatic Cu(II)-carboxylate complex reported in the literature (Tar *et al*., 2025).

Copyright © 2026, Universitas Sebelas Maret, ISSN 1412-4092, e ISSN 2443-4183

Molecular Electrostatic Potential Map

The Molecular Electrostatic Potential Map (MEP) is a useful visualization tool for mapping a molecule's electronic charge distribution and predicting reactive sites for electrophilic and nucleophilic attack (Akbari *et al*., 2024). In the Cu(II) complex with 3-hydroxybenzoic acid (3HBA), the MEP map (Figure 6) shows a significant difference in the distribution of surface charges, which is represented using a color scale where red indicates areas with negative electrostatic potential (electron-rich/nucleophilic), and blue indicates regions with positive electrostatic potential (electron-poor/electrophilic).

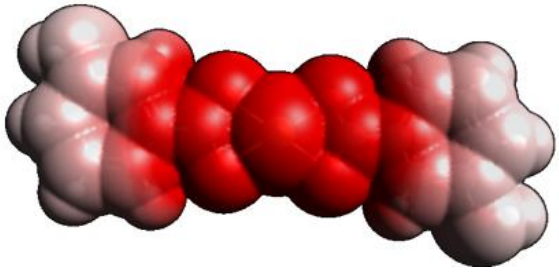


Figure 6. Visualization of the Molecular Electrostatic Potential (MEP) Cu(II) complex with 3HBA.

In this complex, the molecular center involving the copper (Cu) atoms and the carboxylate oxygen atoms is dominated by red, indicating a high negative potential. This indicates that this area has a high electron density and is most likely to interact as an electron or nucleophile donor with positively charged species (electrophiles). The presence of deprotonated carboxylate groups and oxygen atoms coordinating to the electronegative Cu(II) strongly contributes to the accumulation of negative charge at the center of the complex.

The accumulation of negative charges at the coordination center of the metal and carboxylate groups is consistent with the strong electron donor properties of the ionized carboxylate group. This is also in line with the HOMO analysis, which shows that the highest electron density is in the ligand. These sites with high negative potential will be prime targets for interactions with positively charged or electron-deficient substrates in catalytic reactions.

In contrast, the outermost areas of the molecule, especially the benzene ring and the terminal hydrogen atoms bound to carbon, show a color closer to white or pale pink, indicating a less negative or even close to zero, or slightly positive charge. These areas tend to be more stable or neutral and are less attractive sites for electrophilic attack than the complex's center. The more neutral charge distribution in the aromatic ring indicates that the benzene ring's delocalized π system has a relatively even charge density.

CONCLUSION

The complex in this study was successfully synthesized by refluxing $CuCl_2 \cdot 2H_2O$ along with 3-hydroxybenzoic acid (3HBA) at a molar ratio of 1:2. The complex formula is $[Cu(3\text{-hydroxybenzoate})_2]Cl \cdot 24H_2O$, in which Cl^- acts as a counterion. The complex exhibits a single electronic absorption peak at 914 nm, indicating ligand-metal charge-transfer (LMCT) and d-d transitions, consistent with a distorted planar square geometry. The infrared spectrum shows the phenolic –OH band, indicating that –OH is not deprotonated. Computational methods are used to reveal electronic structures and molecular geometries and to verify experimental data. Computational DFT studies of Cu(II) complexes with 3-hydroxybenzoate reveal important electronic structures and molecular geometries. The complex forms a distorted planar square structure with four oxygen atoms from two ligands, with a Cu–O bond length of about 2 Å, signaling a strong coordination interaction. The HOMO-LUMO analysis showed an energy gap of 4.772 eV, indicating moderate kinetic stability and controlled reactivity. HOMO is localized on aromatic ligands, whereas LUMO is centered on the metal and oxygen, exhibiting LMCT transitions relevant to photochemical and catalytic activity. The molecular electrostatic potential (MEP) map highlights the metal center and carboxylate group as the main nucleophilic sites. At the same time, the aromatic ring shows a neutral charge distribution, which is important for understanding non-covalent interactions and for catalysis or molecular recognition applications.

SUPPLEMENTARY FILE

Tables S1 and S2 are available in the Supplementary Information, accessible via the link https://jurnal.uns.ac.id/alchemy/article/view/114305/supp.info.

Copyright © 2026, Universitas Sebelas Maret, ISSN 1412-4092, e ISSN 2443-4183

CONFLICT OF INTEREST

There are no conflicts of interest in this article.

AUTHOR CONTRIBUTION

FK: Writing Original Draft, Methodology, Formal Analysis, Data Curation, Conceptualization; MDJC: Visualization, Software; SBR: Supervision, Funding Acquisition, Conceptualization; TK: Review, Manuscript Editing.

ACKNOWLEDGEMENT

The author would like to express his gratitude to Sebelas Maret University for the financial assistance through the PKGR-UNS grant scheme in 2026.

REFERENCES

Akbari, Z., Stagno, C., Iraci, N., Efferth, T., Omer, E.A., Piperno, A., Montazerozohori, M., Feizi-Dehnayebi, M., and Micale, N., 2024. Biological Evaluation, DFT, MEP, HOMO-LUMO Analysis and Ensemble Docking Studies of Zn(II) Complexes of Bidentate and Tetradentate Schiff Base Ligands as Antileukemia Agents. *Journal of Molecular Structure*, 1301, 137400. https://doi.org/10.1016/j.molstruc.2023.137400.

Aly, S.A., Hassan, S.S., El-Boraey, H.A., Eldourghamy, A., Abdalla, E.M., Alminderej, F.M., and Elganzory, H.H., 2024. Synthesis, Biological Activity, and the Effect of Ionization Radiation on the Spectral, XRD, and TGA Analysis of Cu(I), Cu(II), Zn(II), and Cd(II) Complexes. *Arabian Journal for Science and Engineering*, 49, 361–379. https://doi.org/10.1007/s13369-023-07988-2.

Amin, M.A., Diker, H., Şahin, O., Varlikli, C., and Soliman, A.A., 2025. New Copper and Cobalt Complexes Based on a Fluorinated Pyrazole Derivative, Synthesis, Characterization and Antibacterial Activity. *Applied Organometallic Chemistry*, 39. https://doi.org/10.1002/aoc.70140.

Ashouri, F., Faraji, A.R., Molaeian, S., Fall, M.A., and Butcher, R.J., 2020. The Novel Cobalt and Manganese Polymeric Complex with the Non-Steroidal Anti-Inflammatory Drug Diclofenac: Synthesis, Characterization and Antibacterial Studies. *Journal of Molecular Structure*, 1204, 127483. https://doi.org/10.1016/j.molstruc.2019.127483.

Azizah, N.A.N., Hening Citra Dewi, M., Rahardjo, S.B., and Marliyana, S.D., 2025. Synthesis and Antibacterial Testing of Cu(II)-3-Picolylamine Complexes. *Jurnal Kimia Sains dan Aplikasi*, 28, 267–273. https://doi.org/10.14710/jksa.28.5.267-273.

Becke, A.D., 1993. Density-Functional Thermochemistry. III. The Role of Exact Exchange. *The Journal of Chemical Physics*, 98, 5648–5652. https://doi.org/10.1063/1.464913.

Bhaskar, R.S., Ladole, C.A., Salunkhe, N.G., Barabde, J.M., and Aswar, A.S., 2020. Synthesis, Characterization and Antimicrobial Studies of Novel ONO Donor Hydrazone Schiff Base Complexes with Some Divalent Metal (II) Ions. *Arabian Journal of Chemistry*, 13, 6559–6567. https://doi.org/10.1016/j.arabjc.2020.06.012.

Bhowmick, A., Islam, M., Bhowmick, R., Sarkar, M., Shibly, A., and Hossain, E., 2019. Synthesis and Structure Determination of Some Schiff Base Metal Complexes with Investigating Antibacterial Activity. *American Journal of Chemistry*, 2019. https://doi.org/10.5923/j.chemistry.20190901.03.

Cota, I., Marturano, V., and Tylkowski, B., 2019. Ln Complexes as Double Faced Agents: Study of Antibacterial and Antifungal Activity. *Coordination Chemistry Reviews*, 396, 49–71. https://doi.org/10.1016/j.ccr.2019.05.019.

Devi, J., Yadav, M., Kumar, Anil, and Kumar, Ashwani, 2018. Synthesis, Characterization, Biological Activity, and QSAR Studies of Transition Metal Complexes Derived from Piperonylamine Schiff Bases. *Chemical Papers*, 72, 2479–2502. https://doi.org/10.1007/s11696-018-0480-0.

Domán, A., Madarász, J., and László, K., 2017. In Situ Evolved Gas Analysis Assisted Thermogravimetric (TG-FTIR and TG/DTA–MS) Studies on Non-Activated Copper Benzene-1,3,5-Tricarboxylate. *Thermochimica Acta*, 647, 62–69. https://doi.org/10.1016/j.tca.2016.11.013.

El-Deen, I.M., Shoair, A.F., and El-Bindary, M.A., 2018. Synthesis, Structural Characterization, Molecular Docking and DNA Binding Studies of Copper Complexes. *Journal of Molecular Liquids*, 249, 533–545. https://doi.org/10.1016/j.molliq.2017.11.072.

Ermiş, E., and Durmuş, K., 2020. Novel Thiophene-Benzothiazole Derivative Azomethine and Amine Compounds: Microwave Assisted Synthesis, Spectroscopic Characterization, Solvent Effects on UV–Vis

Copyright © 2026, Universitas Sebelas Maret, ISSN 1412-4092, e ISSN 2443-4183

Absorption and DFT Studies. *Journal of Molecular Structure*, 1217, 128354. https://doi.org/10.1016/j.molstruc.2020.128354.

Grau, J., Montpeyó, D., Lorenzo, J., Roubeau, O., Caubet, A., and Gamez, P., 2024. Square-Planar Copper(II) Complexes from a Zwitterionic Schiff-Base $N_2/N_{2/2}$ -Donor Ligand: DNA Interaction and Cytotoxicity. *European Journal of Inorganic Chemistry*, 27. https://doi.org/10.1002/ejic.202400159.

Grimme, S., Antony, J., Ehrlich, S., and Krieg, H., 2010. A Consistent and Accurate *Ab Initio* Parametrization of Density Functional Dispersion Correction (DFT-D) for the 94 Elements H-Pu. *The Journal of Chemical Physics*, 132. https://doi.org/10.1063/1.3382344.

Grimme, S., Ehrlich, S., and Goerigk, L., 2011. Effect of the Damping Function in Dispersion Corrected Density Functional Theory. *Journal of Computational Chemistry*, 32, 1456–1465. https://doi.org/10.1002/jcc.21759.

Hasanova, S.S., Yolchueva, E.A., Mashadi, A.Q., Muhammad, S., Ashfaq, M., Muhammed, M.E., Munawar, K.S., Tahir, M.N., Al-Sehemi, A.G., and Alarfaji, S.S., 2023. Synthesis, Characterization, Crystal Structures, and Supramolecular Assembly of Copper Complexes Derived from Nitroterephthalic Acid along with Hirshfeld Surface Analysis and Quantum Chemical Studies. *ACS Omega*, 8, 8530–8540. https://doi.org/10.1021/acsomega.2c07686.

Huang, Y., Rong, C., Zhang, R., and Liu, S., 2017. Evaluating Frontier Orbital Energy and HOMO/LUMO Gap with Descriptors from Density Functional Reactivity Theory. *Journal of Molecular Modeling*, 23, 3. https://doi.org/10.1007/s00894-016-3175-x.

Juliá, F., 2022. Ligand-to-Metal Charge Transfer (LMCT) Photochemistry at 3d-Metal Complexes: An Emerging Tool for Sustainable Organic Synthesis. *ChemCatChem*, 14, e202200916. https://doi.org/10.1002/cctc.202200916.

Kargar, H., Ardakani, A.A., Tahir, M.N., Ashfaq, M., and Munawar, K.S., 2021. Synthesis, Spectral Characterization, Crystal Structure Determination and Antimicrobial Activity of Ni(II), Cu(II) and Zn(II) Complexes with the Schiff Base Ligand Derived from 3,5-Dibromosalicylaldehyde. *Journal of Molecular Structure*, 1229, 129842. https://doi.org/10.1016/j.molstruc.2020.129842.

Karges, J., Stokes, R.W., and Cohen, S.M., 2021. Metal Complexes for Therapeutic Applications. *Trends in Chemistry*, 3, 523–534. https://doi.org/10.1016/j.trechm.2021.03.006.

Krishnan, R., Binkley, J.S., Seeger, R., and Pople, J.A., 1980. Self-Consistent Molecular Orbital Methods. XX. A Basis Set for Correlated Wave Functions. *The Journal of Chemical Physics*, 72, 650–654. https://doi.org/10.1063/1.438955.

Lee, C., Yang, W., and Parr, R.G., 1988. Development of the Colle-Salvetti Correlation-Energy Formula into a Functional of the Electron Density. *Physical Review B*, 37, 785–789. https://doi.org/10.1103/PhysRevB.37.785.

Matović, Z.D., Ristić, B., Joksović, M., Trifunović, S.R., Pelosi, G., Ianelli, S., and Ponticelli, G., 2000. Square-Planar Copper(II) Complexes with a Novel Tetradentate Amido-Carboxylate Ligand. Crystal Structure of [Co(H2O)6][Cu(Mda)] · 2H2O. *Transition Metal Chemistry*, 25, 720–726. https://doi.org/10.1023/A:1007051908027.

May, A.M., and Dempsey, J.L., 2024. A New Era of LMCT: Leveraging Ligand-to-Metal Charge Transfer Excited States for Photochemical Reactions. *Chemical Science*, 15, 6661–6678. https://doi.org/10.1039/D3SC05268K.

Miar, M., Shiroudi, A., Pourshamsian, K., Oliaey, A.R., and Hatamjafari, F., 2021. Theoretical Investigations on the HOMO–LUMO Gap and Global Reactivity Descriptor Studies, Natural Bond Orbital, and Nucleus-Independent Chemical Shifts Analyses of 3-Phenylbenzo[*d*]Thiazole-2(3 *H*)-Imine and Its *Para* -Substituted Derivatives: Solvent and Substituent Effects. *Journal of Chemical Research*, 45, 147–158. https://doi.org/10.1177/1747519820932091.

Mohamed, A., Visco, D.P., Breimaier, K., and Bastidas, D.M., 2025. Effect of Molecular Structure on the B3LYP-Computed HOMO–LUMO Gap: A Structure −Property Relationship Using Atomic Signatures. *ACS Omega*, 10, 2799–2808. https://doi.org/10.1021/acsomega.4c08626.

Neese, F., 2012. The ORCA Program System. *WIREs Computational Molecular Science*, 2, 73–78. https://doi.org/10.1002/wcms.81.

Neese, F., Beyer, B. C., Petrenko, T., Pollak, D., and Wennmohs, F., 2020. The ORCA program system: Version 6.1.0. *SoftwareX*.

Ostellari, P., Tapparelli, M., Bragaggia, G., Sandon, A., Lavagnolo, M.C., Girardi, L., Manica, M., Salmaso, L., and Gross, S., 2025. Hydroxy-Carboxylic Acids as Green and Abundant Ligands for Sustainable Recovery of Copper from a Multimetallic Powder: A Proof of Concept. *ChemSusChem*, 18, e202401389. https://doi.org/10.1002/cssc.202401389.

Copyright © 2026, Universitas Sebelas Maret, ISSN 1412-4092, e ISSN 2443-4183

Rasyda, Y.A., Widowati, M.K., Marliyana, S.D., and Rahardjo, S.B., 2021. Synthesis, Characterization and Antibacterial Properties of Nickel(II) Complex with 4-Aminoantipyrine Ligand. *Indonesian Journal of Chemistry*, 21, 391–399. https://doi.org/10.22146/ijc.56552.

Sabolović, J., and Liedl, K.R., 1999. Why Are Copper(II) Amino Acid Complexes Not Planar in Their Crystal Structures? An Ab Initio and Molecular Mechanics Study. *Inorganic Chemistry*, 38. https://doi.org/10.1021/ic980471a.

Tar, H., Alhomaidan, L.M., Beji, L., Alnafisah, A.S., Kouki, N., Messaoudi, S., Alminderej, F.M., Algreiby, A.A., and Aroua, L.M., 2025. Electronic and Photophysical Properties of Copper (II) Complexes: Insights into Solvatochromic Effects, Photoreduction, and Fluorescence Behavior. *Results in Chemistry*, 13, 101957. https://doi.org/10.1016/j.rechem.2024.101957.

Weigend, F., 2006. Accurate Coulomb-Fitting Basis Sets for H to Rn. *Physical Chemistry Chemical Physics*, 8, 1057–1065. https://doi.org/10.1039/b515623h.

Weigend, F., and Ahlrichs, R., 2005. Balanced Basis Sets of Split Valence, Triple Zeta Valence and Quadruple Zeta Valence Quality for H to Rn: Design and Assessment of Accuracy. *Physical Chemistry Chemical Physics*, 7, 3297. https://doi.org/10.1039/b508541a.

Valach, F., Grobelny, R., Glowiak, T., Mrozinski, J., Lukeš, V., and Blahová, Z., 2010. Structural Study of Semi-Coordination in A Seven-Coordinate Copper (II) Complex: Distortion Isomerism of [$Cu(CH_3COO)_2$(4-aminopyridine)$_2$(H_2O)]. *Journal of coordination chemistry*, 63, 1645–1651. https://doi.org/10.1080/00958972.2010.489204.

Yadav, R.B., Kulkarni, N., Mishra, A., Thakkar, A.B., Sargara, P., and Thakkar, S., 2025. Synthesis, Characterization, Antibacterial Properties and in Silico Molecular Docking of Binuclear Copper(II) Complexes with Planar Aromatic Derivatives of Aroyl Hydrazine Ligands. *Journal of the Iranian Chemical Society*, 22, 641–655. https://doi.org/10.1007/s13738-025-03176-1.

Copyright © 2026, Universitas Sebelas Maret, ISSN 1412-4092, e ISSN 2443-4183